

Flexural Behavior of High-Strength Concrete Beams Confined with Stirrups in Pure Bending Zone

Il-Young Jang,^{1)*} Hoon-Gyu Park,²⁾ Yong-Gon Kim,³⁾ Sung-Soo Kim,⁴⁾ and Jong-Hoe Kim⁵⁾

(Received May 18, 2007, Revised June 5, 2008, Accepted February 25, 2009)

Abstract: The purpose of this study is to establish flexural behavior of high-strength concrete beams confined in the pure bending zone with stirrups. The experiment was carried out on full-scale high-strength reinforced concrete beams, of which the compressive strengths were 40 MPa and 70 MPa. The beams were confined with rectangular closed stirrups. Test results are reviewed in terms of flexural capacity and ductility. The effect of web reinforcement ratio, longitudinal reinforcement ratio and shear span to beam depth ratio on ductility are investigated. The analytic method is based on finite element method using fiber-section model, which is known to define the behavior of reinforced concrete structures well up to the ultimate state and is proven to be valid by the verification with the experimental results above. It is found that confinement of concrete compressive regions with closed stirrups does not affect the flexural strength but results in a significantly increased ductility. Moreover, the ductility tends to increase as the quantity of stirrups increases by reducing the spacing of stirrups.

Keywords: high strength, ductility, stirrup, pure span.

1. Introduction

It is recommended to use less reinforced beams in design stage to obtain satisfactory ductility so that adequate warning can be given prior to the failure of the member.^{1,2} When using high-strength concrete, it becomes more brittle if its compressive strength is increased. Thus, it has an inherent disadvantage of inadequate ductility of the member. Because of brittleness, the use of high-strength concrete can be rather inefficient and uneconomical in terms of the flexural capacity if its tensile reinforcement ratio is lowered.

There have been much research to enhance the flexural capacity of high-strength concrete beam members for a long time. In addition, as it has been reported in many researches on beam members, the ductility and flexural capacity can be enhanced when stirrups with appropriate spacing are confined in flexural region of the member. Moreover, transverse reinforcing bars placed in flexural compressive region can greatly improve the deflection ductil-

ity of the beam members.³ This is because the transverse reinforcing bars in the flexural region can effectively resist the tensile stress caused by the expansion of the concrete in the flexural compressive region. Thus, it can be an important data for securing the ductility of high-strength concrete to delineate the flexural behavior of the high-strength concrete in pure bending region in response to the spacing of the transverse reinforcing bar and to establish the relationship between tensile reinforcement ratio and transverse reinforcement ratio of the high-strength concrete. This research investigated the confinement effect of the high-strength concrete through analytical and experimental studies in order to examine the possibility of securing its ductility with transverse reinforcement bars. Additionally, an experiment to quantify the relationship between maximum tensile reinforcement ratio and transverse reinforcement ratio has been performed.

2. Experiment

2.1 Overview

Figure 1 shows the details (shape, size, and layout) of the beam test specimen, which was prepared to investigate the confinement effect in the pure flexural (bending) zone on the flexural behavior of the high-strength concrete beam. Table 1 summarizes the properties of the test specimens and test results.

The target compressive strengths were set at 40 MPa and 70 MPa, and the concrete mixing proportion is shown in Table 2. The specification for the beam member specimen was planned to be cross sectional height of 260 mm (effective height $d=210$ mm), width of 140 mm, tensile reinforcement ratio to balance reinforcement ratio of 50, 75, and 120%. A flexural failure was induced by the stirrup spacing (s) of 100 mm ($0.5d$) pursuant to the ACI code⁴

¹⁾KCI Member, Dept. of Civil Engineering, Kumoh National University of Technology, Gumi 730-701, Korea. E-mail: jbond@kumoh.ac.kr

²⁾KCI Member, LIG Engineering & Construction Co., Ltd., Seoul 135-934, Korea.

³⁾KCI Member, Dept. of Safety Engineering, Hankyong National University, Ansong 456-949, Korea.

⁴⁾Samsung Construction Corporation, Seoul 137-857, Korea.

⁵⁾Ministry of Land Transport and Maritime Affairs, Gwacheon 427-712, Korea.

Copyright © 2009, Korea Concrete Institute. All rights reserved, including the making of copies without the written permission of the copyright proprietors.

Table 1 Properties of test specimens and test results

No.	Beam ID.	f_c (MPa)	Section $b \times d$ (cm)	a/d	Tension steel		Confinement in pure bending zone				P_{cr} (kN)	Yield state		Maximum state		Ultimate state		ϵ_{cu}	μ			
					Size	ρ_t (%)	ρ_b	Size	s (cm)	ρ_w (%)		Shape	P_y (kN)	δ_y (mm)	P_{max} (kN)	δ_{max} (mm)	P_u (kN)			δ_u (mm)		
1	4B4-0.5(0)	41	14×21	4	2D19	1.952	0.562	D10	0	0	9.80	106.43	7.86	120.64	13.90	97.12	28.41	0.0057	2.99			
2	4B4-0.5(10)		14×21		2D19	1.952	0.562		10	1.021	24.60	113.09	10.43	115.25	14.60	93.00	39.13	0.0047	3.75			
3	4B4-0.7(10)		14×21		2D22	2.633	0.758		10	1.021	14.70	143.77	10.55	149.55	13.54	119.36	26.23	0.0049	2.49			
4	4B4-0.7(5)		14×21		2D22	2.633	0.758		5	2.043	14.70	146.12	11.24	148.57	11.87	118.78	33.30	0.0073	3.13			
5	4B4-1.0(10)		14×19.5		4D19	4.205	1.211		10	1.021	19.40	153.86	9.33	184.63	13.17	152.68	19.14	0.0048	2.05			
6	4B4-1.0(5)		14×19.5		4D19	4.205	1.210		5	2.043	13.72	149.35	9.01	181.79	13.80	153.57	23.31	0.0042	2.58			
7	7B4-0.5(0)		71		14×21	4	2D22		2.633	0.502	D10	0	0	18.13	162.58	12.79	165.03	14.79	133.18	30.06	0.0036	2.35
8	7B4-0.5(10)				14×21		2D22		2.633	0.502		10	1.021	23.32	147.78	10.49	163.56	16.06	133.28	35.73	0.0039	3.41
9	7B4-0.7(10)				14×19.5		4D19		4.205	0.803		10	1.021	29.40	200.41	12.95	200.70	13.49	159.64	25.02	0.0070	1.93
10	7B4-0.7(5)				14×19.5		4D19		4.205	0.803		5	2.043	24.50	211.88	13.58	212.37	13.76	174.15	27.43	0.0034	2.02

(Note) P_y and δ_y = load and displacement at yielding point of tension steel, P_u and δ_u = load and displacement at 0.8 P_{max} after peak, μ = displacement ductility ($=\delta_u / \delta_y$).

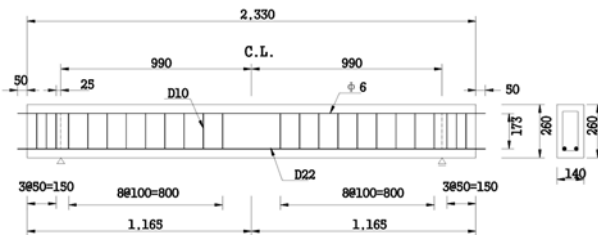


Fig. 1 Detail of test specimens.

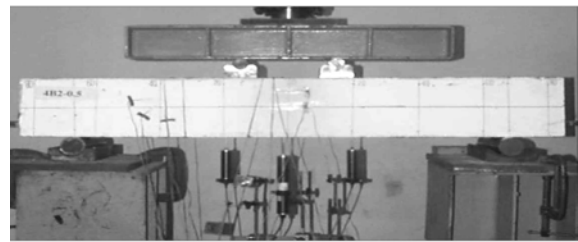


Fig. 2 Loading test set-up.

Table 2 Mix of high-strength concrete.

Target compressive strength at 28 days (MPa)	40	70
W/B	0.480	0.250
S/a	0.437	0.390
Water (kg/m ³)	180	160
Cement (kg/m ³)	375	608
Gravel (kg/m ³)	997	1008
Sand (kg/m ³)	765	622
Silica fume (kg/m ³)	0	32
Super-plasticizer (kg/m ³)	0.43	2.33

throughout the entire section, and transverse reinforcing bars, which were composed of closed stirrups and an important experimental variable of this study, were laid out at the spacing of none, 50 mm (0.25d), 100 mm (0.5d) in pure bending zone. The steel bar type D10 was used for the stirrups and transverse reinforcing bars, deformed reinforcing bars of 6 mm were installed in the compressive side for the location fixation. deformed reinforcing bars of 6 mm were installed in the compressive side for the location fixation. The closed stirrups were made of standard 90° hook.

All experiments used the loading frame for structural testing as shown in Fig. 2, and the loading was applied by a load cell of 100 kN capacity. The load was supported by hinges at both ends of the beam, and four point loading was applied while maintaining the spacing of 300 mm between the loading points through H150 × 150 × 7 × 10 mm steel.

The loading was controlled to increase the load uniformly up to 1/3 of the failure load, and, afterwards, it was applied by displacement control from the deflection measured through a LVDT

installed at the center of the test specimen. While the loading is applied, three LVDT's installed at the center and both sides 200 mm away from the center measured the deflection of the beam. Additionally, the concrete compressive strain in pure flexural zone and the strain of the reinforcement bars including tensile reinforcement bars and closed stirrups, were measured.

2.2 Material test

The results of tensile strength of the steel and compressive strengths of the concrete are shown in Tables 3 and 4, respectively.

Table 3 Mechanical properties of steel.

Steel size	Yield strength (MPa)	Ultimate strength (MPa)	Yield strain	Modulus of elasticity (MPa)	Elongation (%)
D10	395.0	592.4	0.002054	192350	23.4
D19	435.1	617.9	0.002064	210760	21.2
D22	450.1	619.0	0.002042	220450	19.5

Table 4 Properties of concrete.

Properties			Target compressive strength (MPa)	
			40	70
Fresh	Slump	mm	160	150
	Age	Day	28	28
Hardened	f_c	MPa	41	71
	E_c	MPa	27,463	32,710

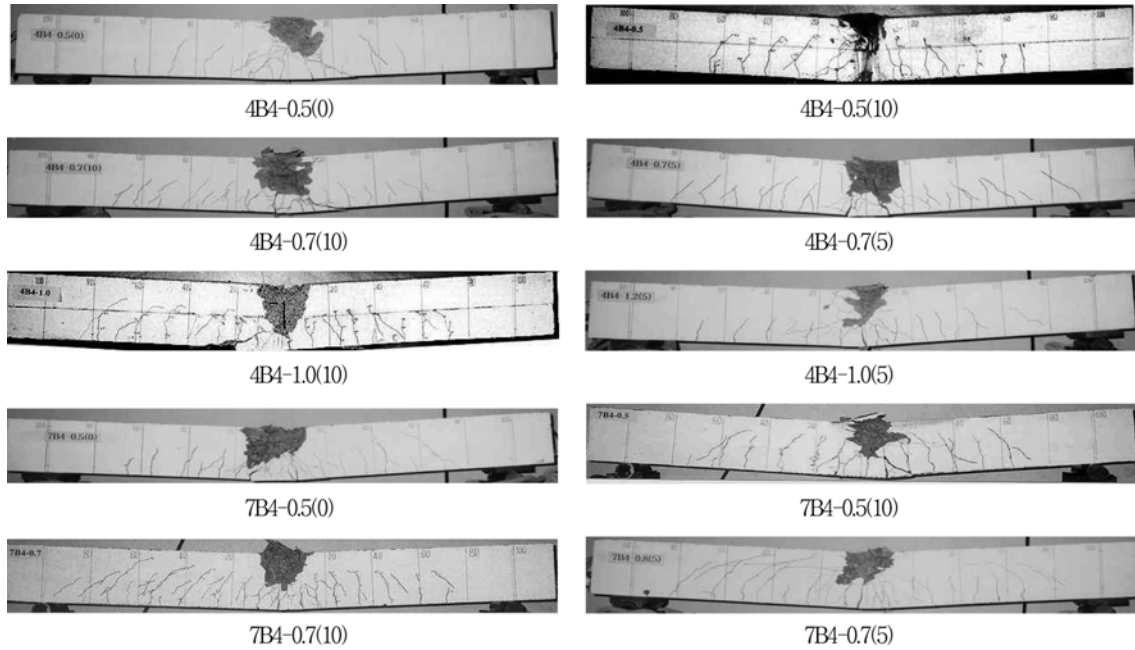


Fig. 3 Crack propagation and failure pattern.

3. Experimental result

3.1 Crack propagation and failure mode

Figure 3 shows the crack propagation and failure mode of the beam test specimens. The vertical cracking took place from the bottom of the beam in which pure bending (flexural) stress occurred and propagated vertically. The initial flexural cracking occurred between the loading points in pure bending zone. Most of the crack spacing were between 70~100 mm. The crack spacing was narrow and complex, and a sudden failure was observed after the failure of the concrete in the compressive side subsequent to the yield of tensile steel in pure bending zone.

3.2 Load-deflection relationship

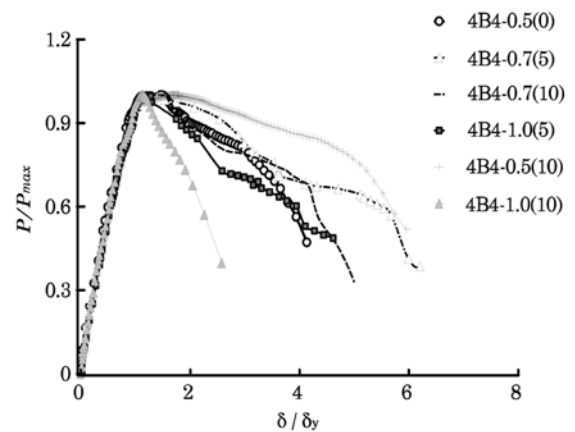
The strengths of the test specimens were compared in Fig. 4 to investigate the flexural capacity of the specimen in pure bending zone by the normalized load-deflection relationship.

The maximum load maintained the same strength regardless of the spacing of the stirrups in the plastic hinge zone. On the contrary, the flexural ductility (δ_u / δ_y) of the concrete beam member increased by 1.3 to 1.5 times as the spacing of the stirrups in its pure bending zone became narrowed.

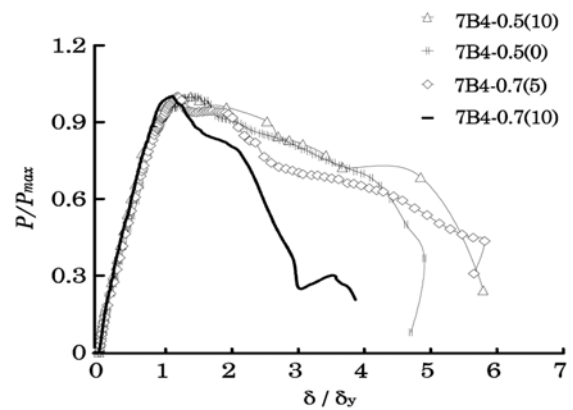
3.3 Compressive strain on the reinforcing bar

Attainment of appropriate ductility is possible with enhanced bending capacity by confining the lateral expansion of the concrete in pure bending zone with stirrups. Thus, strain gauges were installed at the center, top part, and corner as shown in Fig. 5 in order to investigate the confinement effect in the pure bending zone by the stirrups. Fig. 6 depicts the load-strain relationship of the stirrups for the representative test specimens, 4B4-0.7(10) and 4B4-0.5(0).

The 4B4-0.7(10) test specimen showed that the strain (displacement) at the corner of the stirrup is a little greater than that at the top part or the center up to the maximum load as shown in the



(a) Load-deflection relationship of 400 MPa test specimens



(b) Load-deflection relationship of 700 MPa test specimens

Fig. 4 Comparison of normalized load-deflection.

load-strain curve of the figure. Then, the strain at the corner became greater after the maximum load. The 4B4-0.5(0) test specimen showed almost same behavior up to the maximum load, and

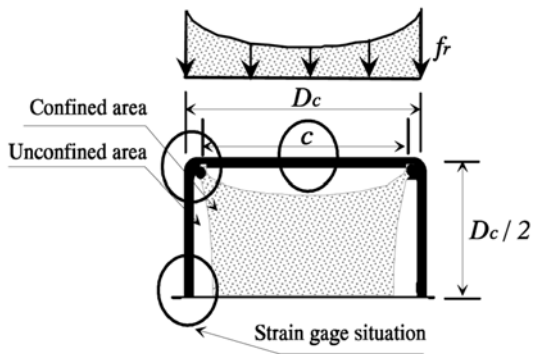


Fig. 5 Lateral pressure in tied square beams.

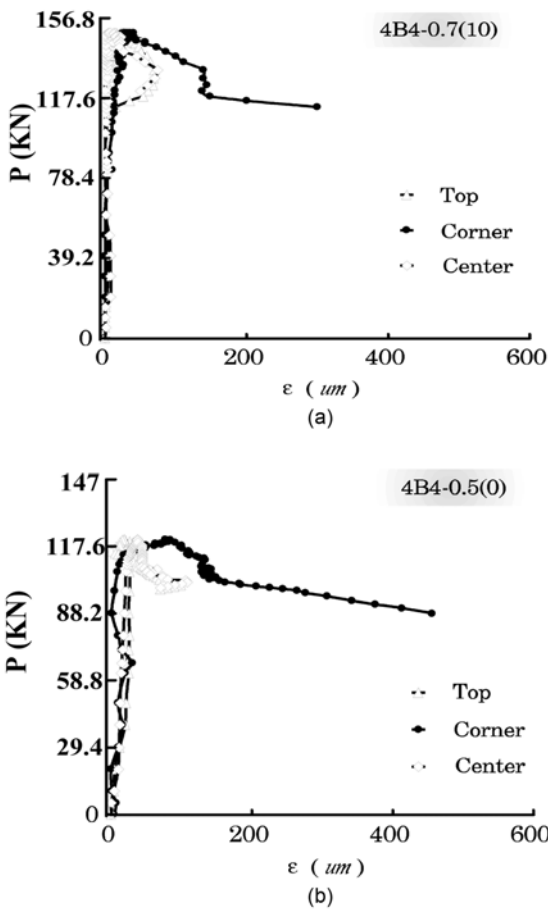


Fig. 6 Relations of $P-\varepsilon$ at various locations of the stirrup.

the stain at the corner of the stirrup manifested greater value after the maximum load. This manifestation of greater strain at the corner of the stirrup means that stress is concentrated in the corner of the stirrup.

4. Analysis of the behavior of beam member in consideration of confinement effect

4.1 Analysis process

This study carried out moment-curvature analysis using a relatively simple but reasonably accurate layer model in order to investigate the high-strength concrete structural member up to the ultimate state.⁶

Because the ductility behavior from the analytical results at the maximum load and after the maximum load can change by the length of the member element, the length of the member element was partitioned by the expected length of the plastic hinge (about $d/2$). Considering the symmetry of the beam member, only the half of the entire length of the member was modeled for the analysis. Additionally, the analysis was carried out for the state of stirrup confinement and the state of no such confinement.

4.2 Discussion on the analysis result

The results of the comparison of moment-curvature and load-deflection by the layer model are shown in Figs. 7 and 8, respectively. It is evaluated that the load-deflection behavior of the high-strength concrete beam by tensile reinforcement ratio, shear-span to beam depth ratio is well explained by these analysis results. The initial stiffness, yielding the member, maximum strength, and the behavior after the maximum loading, which is the most influential factors in evaluating the ductility of the member, coincided well with the experimental results.

5. Proposal for the spacing of stirrup confinement by the tensile reinforcement ratio

The experimental results discussed in the previous section 3 for

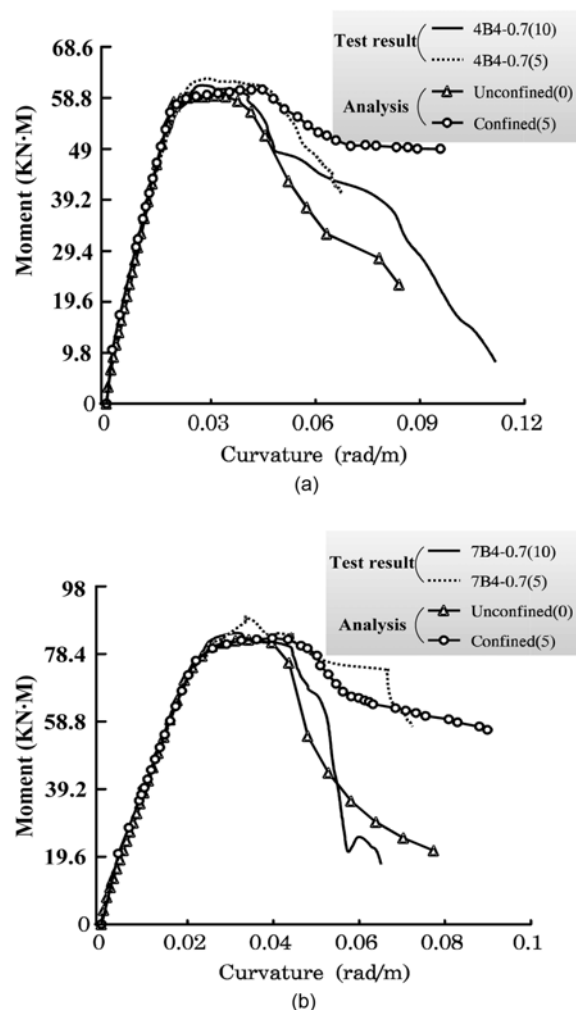


Fig. 7 Comparison of moment-curvature.

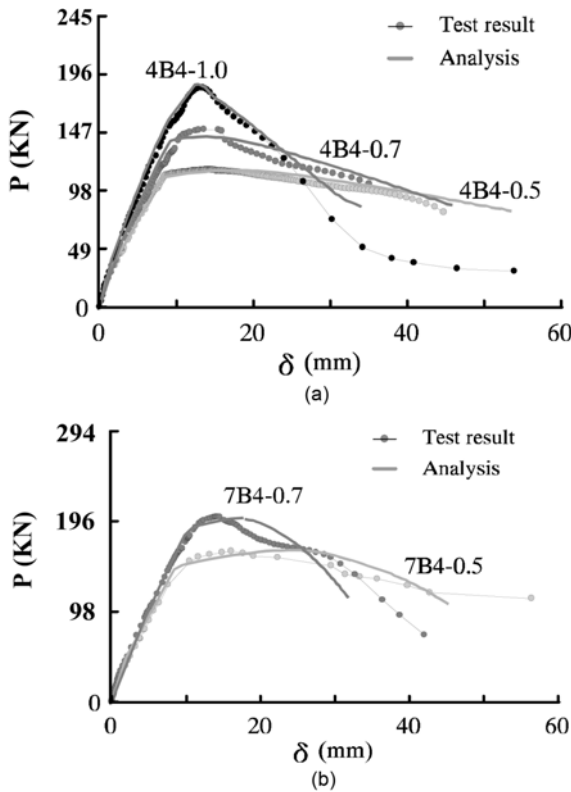


Fig. 8 Comparison of load-deflection.

the closely spaced layout of stirrups (from the analysis of this experiment, $s \leq 0.48d$) indicate that the ductility of the member is greatly enhanced. This implies that, if stirrups are properly laid out to the plastic hinge area within the bending zone of the concrete beam member, the ductility can be increased even without the reduction in the tensile reinforcement ratio. The concrete beam member reinforced with closely spaced stirrups in pure bending zone can greatly enhance the moment-rotation capacity. Thus, an examination of the amount of tensile reinforcement is necessary in consideration of the ductility enhancement with the stirrup reinforcement.

The compressive force (C) resisted by the concrete, when the maximum compressive strain reaches the ultimate strain ϵ_{cu} can be obtained from the concrete stress-strain curve and is expressed as the following Eq. (1).

$$C = \alpha f_c b \beta c \quad (1)$$

where c is the distance to the neutral axis, α , the average stress coefficient, is equivalent to $k_3 = 0.85$ of ACI-318 specification on stress block; and β , the centroid coefficient, is the same as β_1 . The α and β of the concrete confined by transverse reinforcement bars such as spiral bar, tie bar, or stirrup are also obtained from stress-strain model and are expressed as in Eqs. (2) and (3), respectively.

$$\alpha = \frac{\int_0^{\epsilon_{oc}} f_{ic} d\epsilon_{ic}}{\epsilon_{oc} f_{oc}} \quad (2)$$

$$\beta = 1 - \frac{\int_0^{\epsilon_{oc}} f_{ic} \epsilon_{ic} d\epsilon_{ic}}{\epsilon_{oc} \int_0^{\epsilon_{oc}} f_{ic} d\epsilon_{ic}} \quad (3)$$

Most of the test specimens showing flexural failure mode by the result of this experiment started to fail from the compressive strain at the concrete between 0.002~0.006. The lateral (transverse) confinement (f_r) increased the compressive strength of the core concrete inside the transverse reinforcement bar after spalling of the cover concrete without the failure of the entire member. Accordingly, this study took the ultimate strain of the confined concrete as the strain (ϵ_{oc}) at the maximum compressive strength (f_{oc}) from Eqs. (2) and (3).

The following Fig. 9 shows the change in the values of α and β in Eqs. (2) and (3) obtained from the stress-strain model for the confined concrete as proposed by Jang I. Y. et. al.⁷ The α and β increased with the increase in the compressive strength ratio (f_{oc}/f_c) in the range of concrete compressive strength between 30 MPa and 100 MPa and the compressive strength ratio increase between 1.05 to 2, and their rate decreased with the increase in compressive strength of the concrete. The average and standard deviation of the α in this range were 0.812 and 3.7%, respectively. The β had the average value of 0.828 and standard deviation of 3.1%.

Table 5 shows the comparison of flexural strength with different spacings of the stirrups. Here, the confinement force (f_r), compressive strength (f_{oc}) and strain (ϵ_{oc}) were computed from the equation proposed by Park H. G.⁶ and M_{um} is the maximum moment obtained from the analysis of moment-curvature based on the stress-strain models for unconfined concrete and confined concrete. The comparison in Table 5 indicates that the test specimens of this study exert greater confinement force as the spacing of the stirrups is closer. If the test specimen has no confinement force and is assumed to be not confined, the test specimen with confinement effect of $f_{oc}/f_c \geq 1$ would have exhibited almost no increase in the strength as evidenced by the experimental result of $M_{test}/M_{um} = 100.4\sim 119.7\%$. Furthermore, the comparison of flexural strength between the unconfined model and confined model revealed almost no increase in the flexural (bending) strength. Thus, as reported by Base³ or Park H. G. et. al.,⁶ the reinforcing stirrups in the bending zone of the beam do not have much effect on increasing the flexural strength of the beam. Thus, it is believed that, even if the entire compressive side in the cross section is assumed to be confined, the assumption will not affect the evaluation of the ultimate strength of the member. Figure 10 shows that this is a relatively acceptable assumption.

The result of moment-curvature analysis for the 4B4-0.5(10) specimen member with the stirrup spacing $s/d = 0.48$ followings as illustrated in Fig. 10. The analysis result shows that the defor-

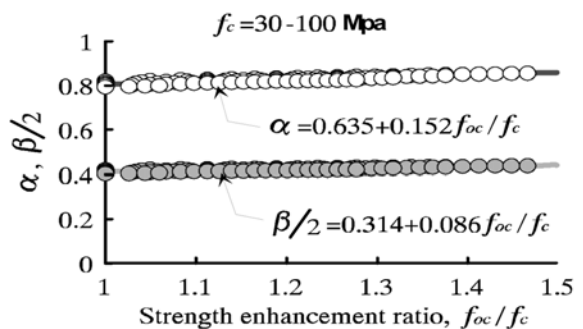


Fig. 9 Comparison of the enhancement ratio (the ratio of increase in compressive strength), f_{oc}/f_c .

Table 5 Flexural capacities of high-strength concrete beams in confinement state.

Beam ID.	f_c	ϵ_{cu}	f_r	ϵ_{oc}	f_{oc}	$\frac{f_{oc}}{f_c}$	M_{test}	M_{un}	$\frac{M_{test}}{M_{un}}$
4B4-0.5(10)	41.0	0.47	1.944	0.00366	43.6336	1.064	4.939	4.765	1.037
4B4-1.0(10)	41.0	0.48	1.944	0.00366	43.6336	1.064	7.912	6.612	1.197
7B4-0.5(10)	71.2	0.39	0.633	0.00342	72.5000	1.018	7.010	6.898	1.016
7B4-0.7(10)	71.2	0.70	0.633	0.00342	72.5000	1.018	8.597	8.419	1.021
4B4-0.7(10)	41.2	0.49	1.944	0.00366	43.6336	1.064	6.245	6.162	1.013
4B4-0.5(0)	41.2	0.57	0.000	0.00237	41.0000	1.000	5.170	4.765	1.085
4B4-0.7(5)	41.2	0.73	7.136	0.00773	48.0000	1.171	6.367	6.163	1.038
4B4-1.0(5)	41.2	0.42	7.136	0.00773	48.0000	1.171	6.644	6.612	1.004
7B4-0.5(0)	71.2	0.36	0.000	0.00285	71.2000	1.000	7.073	6.899	1.025
7B4-0.7(5)	71.2	0.34	1.591	0.00499	73.8000	1.037	9.101	8.068	1.128

(Note) M_{un} is predicted moment by unconfined model

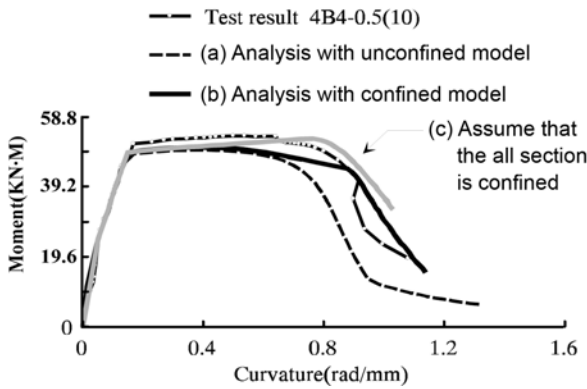


Fig. 10 Comparison between experimental and analytical moment-curvature curves.

mation of the cross section is greatly affected but the flexural (bending) strength is not much affected for the following three cases - (a) unconfined model, (b) the application of stress-strain model for the concrete confined by the stirrups except the concrete cover, and (c) the assumption of the entire cross section as confined concrete. Accordingly, the new equation for evaluation of the tensile steel ratio is suggested as in the following equation.

$$\rho_{bc} = \frac{A_s}{bd} = \frac{\alpha\beta K_s f_{ck} \left[\frac{\epsilon_c E_s}{\epsilon_c E_s + f_y} - \frac{d_1}{d} \right] b'}{f_y} + 0.85 f_{ck} \beta_1 \left[\frac{b' d_1}{bd} - \frac{2b_1}{b} \frac{\epsilon_c E_s}{\epsilon_c E_s + f_y} \right] \quad (4)$$

$$K_s f_{ck} = f_{oc} \quad (5)$$

The Eq. (4) can also be expressed with fewer terms as the following equation.

$$\rho_{bc} = \frac{A_s}{bd} = \frac{\alpha\beta K_s f_{ck}}{f_y} \frac{\epsilon_c E_s}{\epsilon_c E_s + f_y} \quad (6)$$

The relationships between ρ_{bc} and ρ_b as computed by equation for the specimen with appropriate shear reinforcement are summarized in Table 6. However, the analysis of experiment results indicates that the flexural ductility is not greatly enhanced even if the

Table 6 Tension steel ratio for confined concrete beams

Beam ID.	f_c (MPa)	f_{oc}/f_c	ρ_t (%)	ρ_b (%)	ρ_{bc} (%)	ρ_{bc} / ρ_b
4B4-0.5(10)	41.0	1.064	1.952	3.937	4.440	1.090
4B4-1.0(10)	41.0	1.064	4.205	3.937	4.081	1.090
7B4-0.5(10)	71.2	1.018	2.633	5.001	6.415	1.379
7B4-0.7(10)	71.2	1.018	4.205	5.001	6.636	1.379
4B4-0.7(10)	41.0	1.064	2.633	3.937	3.945	1.090
4B4-0.5(0)	41.0	1.000	1.952	3.937	3.152	1.000
4B4-0.7(5)	41.0	1.171	2.633	3.937	6.097	1.545
4B4-1.0(5)	41.0	1.171	4.205	3.937	6.307	1.545
7B4-0.5(0)	71.2	1.000	2.633	5.001	5.745	1.000
7B4-0.7(5)	71.2	1.037	4.205	5.001	8.337	1.621

stirrups in the bending zone is reinforced to 50 mm spacing for the high-strength concrete beam of 70 MPa compressive strength.

This means that adequate enhancement of ductility is difficult to obtain by the stirrup reinforcement in the bending zone for the case of high-strength concrete beams with an excessive reinforcement as is done in this study. Thus, the Eq. (6) needs to be modified in the first place in order to apply the new reinforcement ratio to actual design of the concrete beam with enhanced ductility. The ductility of the reinforced concrete member subjected to pure bending is the most affected by tensile reinforcement ratio. Thus, it would be the most simple method to compute the quantity of steel reinforcement necessary for the attainment of ductility of the member in its structural design by expressing the ductility of the member based on the relationship between tensile reinforcement ratio and balanced reinforcement ratio. Figure 11 compares the analytical results of bending-displacement relationship by the change in tensile reinforcement ratio, the result of this experiment, and typical experimental results from previous researches. All beams were simply reinforced and their compressive strengths were between 26 and 120 MPa. As shown in Fig. 11(a), when specimens with lateral stirrup reinforcement is compared with the specimen, which has no lateral stirrup reinforcement in the bending zone with the specification of $f_{ck} = 50$ MPa, $a/d = 4$, and $\rho_c = 0\%$, their experimental data for variables other than tensile reinforcement ratio are dispersed more. However, the experimental result indicates the general trend of increased ductility index with the increase in ρ_t / ρ_b . It is thus found that the ductility of

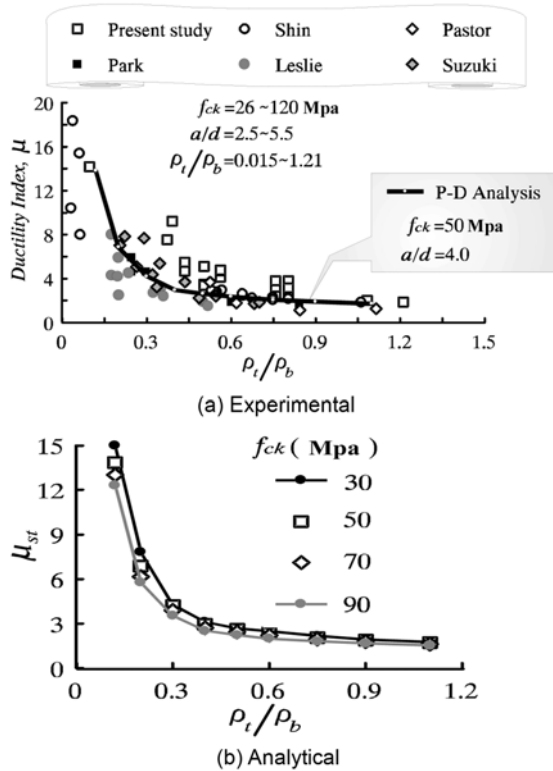


Fig. 11 Effects of ρ_t/ρ_b and f_c on the ductility.

beam members is difficult to evaluate accurately with ρ_t/ρ_b alone as can be seen by the dispersion of the experimental data. The data (Fig. 11(b)) shows the general trend of reduced ductility with the increase in concrete compressive strength, given the same experimental condition of ρ_t/ρ_b . Although the balanced reinforcement, ρ_b , is a function of concrete compressive strength and yield strength of the tensile steel, the compressive strength is only an independent variable here. Thus, it is also found that the ductility index varies with the concrete compressive strength even if ρ_t/ρ_b and all other variables including a/d , ρ_c , ρ_w and cross-sectional dimension are kept the same.

An equation to compute the tensile reinforcement ratio, which can lead to required ductility (μ_{req}) is proposed in the following Eq. (7) based on the analytical and experimental results.

$$\rho_t = 2.04 \left[\frac{1.14 - 0.15 \left(\frac{f_{ck}}{500} \right)}{\mu_{req}} + 1.15 \right]^2 \quad (7)$$

The tensile reinforcement ratio to attain the required ductility index of 3 for the high-strength concrete beam of 70 MPa compressive strength should be $\rho_t \leq 0.43\rho_c$ based on the Eq. (7) above. When the required tensile reinforcement ratio (ρ_{req}), to satisfy the required flexural strength is greater than the tensile reinforcement ratio, ρ_b , (Eq. (7)) to attain the required ductility in designing high-strength concrete beam, stirrups must be placed in the bending zone in order to improve the flexural strength and ductility with the lateral reinforcement effect. Here, the spacing of the stirrups must be less than the maximum spacing of $0.5d$, and the spacing must be adjusted to satisfy the requirement of $\rho_{req} \leq \rho_{bc}$ given in Eq. (7). The required tensile reinforcement ratio, to satisfy the required flexural

strength is computed from the following Eqs. (8) and (9).

$$c = \frac{A_s f_y}{\alpha \beta b' K_s' f_{ck}} \quad (8)$$

$$M = A_s f_y \left(d' - 0.5625 \frac{A_s f_y}{K_s b' f_{ck}} \right) \quad (9)$$

here, c is the distance to the neutral axis of the cross section, and it is assumed that the influence of concrete cover on the transverse (lateral) reinforcement effect is insignificant.

6. Conclusions

The conclusions derived from this experimental study can be summarized as follows.

- 1) It is effective to place the stirrups in the bending zone pertinently in accordance with the tensile reinforcement ratio in order to attain satisfactory flexural strength and ductility of high-strength concrete beams.
- 2) A new analytical equation is proposed in consideration of the enhanced ductility and improved stress-strain behavior of high-strength concrete beams in the bending zone by the stirrup confinement effect.
- 3) A computation equation for the required tensile reinforcement ratio is proposed to result in the attainment of the required ductility of the beam member to bring about the stirrup confinement effect.

Acknowledgement

The work in this paper was funded by "Concrete Korea Research Center (05-CCT-D11)" belonging to Korea Ministry of Construction & Transportation and "Human Resource Training Project for Regional Innovation" supported by Korea Industrial Technology Foundation and the Ministry of Education Science Technology. Their financial supports are gratefully acknowledged.

References

1. Ministry of Construction & Transportation, Concrete Structural Design Standard, 1999.
2. Ministry of Construction & Transportation, Concrete Standard Specification, 2000.
3. Base, G. D. and Read, J. B., "Effectiveness of Helical Binding in the Compression Zone of Concrete Beams," *ACI Journal*, Vol. 62, No. 4, 1965, pp. 763~781.
4. ACI Committee 318, *Building Code Requirements for Reinforced Concrete (ACI 318-95)* ACI, Detroit, 1995.
5. Leslie, K. E., Rajagopalan, K. S., and Eveard, N. J., "Flexural Behavior of High-Strength Concrete Beams," *ACI Journal*, Vol. 73, No. 8, 1976, pp. 517~521.
6. Park, H. G., "Nonlinear Modeling and Ductility Evaluation for High-Strength Concrete Structural Members," Ph.D. Dissertation, Kumoh National University of Technology, 2000.
7. Jang, I. Y. and Park, H. G., "Comparison and Evaluation of Stress-Strain Models for High-Strength and Ultra-Strength Concrete," *Journal of Korea Concrete Institute*, Vol. 9, No. 4, 1997, pp. 177~186.